Supplemental Material
Wave-function hybridization in Yu-Shiba-Rusinov dimers

Michael Ruby,[1] Benjamin W. Heinrich,[1] Yang Peng,[2,3,4] Felix von Oppen,[2] and Katharina J. Franke[1]

[1] *Fachbereich Physik, Freie Universität Berlin, 14195 Berlin, Germany*
[2] *Dahlem Center for Complex Quantum Systems and Fachbereich Physik, Freie Universität Berlin, 14195 Berlin, Germany*
[3] *Institute of Quantum Information and Matter and Department of Physics, California Institute of Technology, Pasadena, CA 91125, USA*
[4] *Walter Burke Institute for Theoretical Physics, California Institute of Technology, Pasadena, CA 91125, USA*

SHIBA STATE WITH A SINGLE MAGNETIC IMPURITY

General Consideration

To generate d-orbital-like Shiba bound states numerically (without attempting to accurately describe the specific system at hand), consider a single magnetic moment embedded in a homogeneous s-wave superconductor, as described by the Bogoliubov–de Gennes Hamiltonian

$$H = H_s + J(r)\sigma_z, \tag{S1}$$

where $J(r)$ is the exchange potential between the magnetic moment and the itinerant electrons of the superconductor. We choose $J(r)$ isotropic and neglect the potential scattering by the impurity for simplicity. Note that we choose the direction of the magnetic moment to be the z direction. The superconductor is described by the Hamiltonian

$$H_s = \left(-\frac{\nabla^2}{2} - \mu\right)\tau_z + \Delta\tau_x. \tag{S2}$$

Here, $\sigma_{x,y,z}$ and $\tau_{x,y,z}$ are Pauli matrices in spin and particle-hole space, respectively, $\Delta > 0$ is the pairing potential and μ the chemical potential. We choose units such that the electron charge e, the electron mass m, and $\hbar$ are all equal to unity.

Since the exchange potential $J(r)$ is isotropic, we use spherical coordinates (r, θ, ϕ) centered at the position of the magnetic moment. The Hamiltonian for the superconductor H_s can be rewritten as

$$H_s = H_r\tau_z + \Delta\tau_x, \tag{S3}$$

with

$$H_r = -\frac{1}{2}\left(\frac{d^2}{dr^2} + \frac{2}{r}\frac{d}{dr} + \frac{l(l+1)}{r^2}\right) - \mu. \tag{S4}$$

where l denotes the angular momentum.

Confining the system to a large sphere with radius R, one has a discrete set of basis functions $\{\rho_{k,l}(r)Y_{l,m}(\theta,\phi)\}$, with spherical Harmonics $Y_{l,m}(\theta,\phi)$ and

$$\rho_{k,l}(r) = \frac{\sqrt{2}}{\sqrt{R^3}} j_l(\alpha_{k,l}\frac{r}{R})/j_{l+1}(\alpha_{k,l}) = \frac{\sqrt{2}}{\sqrt{Rr}} J_{l+\frac{1}{2}}(\alpha_{k,l}\frac{r}{R})/J_{l+\frac{3}{2}}(\alpha_{k,l}). \tag{S5}$$

Here, j_l and J_l are the spherical and cylindrical Bessel function of order l. $j_l(\alpha_{k,l})$ is normalized in the sphere of radius R and $\alpha_{k,l}$ is the kth zero of j_l. We have used the relation

$$j_l(r) = \sqrt{\frac{\pi}{2r}} J_{l+\frac{1}{2}}(r) \tag{S6}$$

in obtaining the above equation.

Since the Hamiltonian is isotropic, it is block-diagonal in the angular-momentum quantum numbers l, m. For each l, m, the Hamiltonian H_s of the superconductor is diagonal in k with matrix elements

$$(H_s)_{k,k'} = \left[(\frac{\alpha_{k,l}^2}{2R^2} - \mu)\tau_z + \Delta\tau_x\right]\delta_{k,k'}. \tag{S7}$$

The exchange potential has matrix elements

$$J_{k,k'} = \int_0^\infty r^2 dr \rho_{k,l}(r)\rho_{k',l}(r)J(r). \tag{S8}$$

To find the Shiba state, we fix $\sigma_z = 1$ and solve the eigenvalue problem with eigenvalue $-\Delta < E < \Delta$. The other solution at the opposite energy follows from $\sigma_z = -1$ and can be obtained by particle-hole symmetry.

Shiba states with $l = 2$

To simulate the Shiba states of Mn adatoms, we consider the $l = 2$ channel. For an adatom located in a completely isotropic environment, there are five degenerate Shiba states with the same radial wavefunction but different angular wavefunctions corresponding to $m = \pm 2, \pm 1, 0$. Instead of complex spherical harmonics, we can pass to the real angular-momentum basis, with

$$Y_{xy} = \frac{i}{\sqrt{2}}\left(Y_{2,-2} - Y_{2,2}\right) \tag{S9}$$

$$Y_{yz} = \frac{i}{\sqrt{2}}\left(Y_{2,-1} + Y_{2,1}\right) \tag{S10}$$

$$Y_{z^2} = Y_{2,0} \tag{S11}$$

$$Y_{xz} = \frac{1}{\sqrt{2}}\left(Y_{2,-1} - Y_{2,1}\right) \tag{S12}$$

$$Y_{x^2-y^2} = \frac{1}{\sqrt{2}}\left(Y_{2,-2} + Y_{2,2}\right). \tag{S13}$$

If we choose the quantization axis along the z-axis, these five wavefunctions have the shape of d_{xy}, d_{yz}, d_{z^2}, d_{xz} and $d_{x^2-y^2}$ orbitals, respectively.

In experiment, the Mn adatom is located on the surface of a superconductor, which reduces the symmetry of the adatom environment to the point group C_{4v}. Thus, the five degenerate Shiba states split due to the crystal field according to the irreproducible representations of C_{4v}. If we take the z-direction along the normal to the surface of the superconductor, the d_{z^2}, $d_{x^2-y^2}$, and d_{xy} states are nondegenerate, while the d_{xz} and d_{yz} are degenerate. Experiment yields only three peaks as the d_{xz}, d_{yz}, and d_{xy} states are close in energy [see Ref.[1]]

SHIBA STATE WITH TWO MAGNETIC IMPURITIES

Variational ansatz for Shiba dimer wavefunction

Now consider a system with two ferromagnetically aligned magnetic impurities embedded in a superconductor. Motivated by our experimental results, we assume that the coupling between the two adatoms is weak compared to the energy separation between the α, β, and γ peaks. In this limit, the wavefunctions of magnetic dimers can be written as linear combinations of Shiba states of the individual impurities.

For two magnetic impurities, the Hamiltonian can be written as

$$H = H_s + J(\boldsymbol{r} - \frac{d}{2}\hat{y})\sigma_z + J(\boldsymbol{r} + \frac{d}{2}\hat{y})\sigma_z, \tag{S14}$$

where d denotes the distance between the two impurities. We choose the dimer axis to be aligned along the y axis. Similar to the discussion for a single impurity, we can fix $\sigma_z = 1$.

When the two magnetic impurities couple, the single-impurity peaks in the STM measurement split due to hybridization of the corresponding single Shiba wavefunctions. Hence, we make the variational ansatz

$$\psi(r) = \sum_j \left\{ c_{1,j}\phi_j(\boldsymbol{r} - \frac{d}{2}\hat{y}) + c_{2,j}\phi_j(\boldsymbol{r} + \frac{d}{2}\hat{y}) \right\}, \tag{S15}$$

for the dimer wavefunction. Here, $\phi_j(\boldsymbol{r})$ is the two component Shiba wave function for a single impurity with $j = z^2, x^2 - y^2, xy, yz, xz$, which satisfies

$$[H_s + J(\boldsymbol{r})]\,\phi_j(\boldsymbol{r}) = E_s\phi_j(\boldsymbol{r}), \quad |E_s| \leq \Delta. \tag{S16}$$

The sum over j refers to the sum over xy, yz, xz for the γ peak, and involves only the $x^2 - y^2$ and z^2 orbitals for the α and β peaks, respectively. The Shiba energy E_s for a single impurity can be obtained numerically following the discussion in the previous section.

Using the variational wave function, we obtain the following generalized eigenvalue equation

$$\begin{pmatrix} E_s\mathbf{1} + \mathbf{C} & E_s\mathbf{S} + \mathbf{D} \\ E_s\mathbf{S} + \mathbf{D} & E_s\mathbf{1} + \mathbf{C} \end{pmatrix} \begin{pmatrix} \mathbf{c}_1 \\ \mathbf{c}_2 \end{pmatrix} = \begin{pmatrix} E\mathbf{1} & E\mathbf{S} \\ E\mathbf{S} & E\mathbf{1} \end{pmatrix} \begin{pmatrix} \mathbf{c}_1 \\ \mathbf{c}_2 \end{pmatrix} \tag{S17}$$

where $\mathbf{S}$, $\mathbf{C}$ and $\mathbf{D}$ are matrices for overlap, Coulomb-like and exchange-like integrals, similar to the integrals describing the chemical bonding of the H_2 molecule. The corresponding matrix elements are given by

$$S_{ij} = \int d\boldsymbol{r}\,\phi_i(\boldsymbol{r})^\dagger\phi_j(\boldsymbol{r} + d\hat{y}) \tag{S18}$$

$$C_{ij} = \int d\boldsymbol{r}\,J(\boldsymbol{r} + d\hat{y})\phi_i^\dagger(\boldsymbol{r})\phi_j(\mathbf{r}) \tag{S19}$$

$$D_{ij} = \int d\boldsymbol{r}\,J(\boldsymbol{r})\phi_i(\boldsymbol{r})^\dagger\phi_j(\boldsymbol{r} + d\hat{y}). \tag{S20}$$

$\mathbf{c}_1$ and $\mathbf{c}_2$ are column vectors with elements $c_{1,j}$ and $c_{2,j}$ respectively, in which j takes values from the relevant subset of the five d states, depending on the degeneracy.

For the nondegerate α and β peaks, the above matrices and vectors are only scalars. We denote theses scalars without their indices for simplicity. By solving the eigenvalue equation, we obtain two Shiba energies

$$E_\pm = E_s + \frac{C \pm D}{1 \pm S} \tag{S21}$$

with wavefunctions

$$\psi = \phi(\boldsymbol{r} - \frac{d}{2}\hat{y}) \pm \phi(\boldsymbol{r} + \frac{d}{2}\hat{y}). \tag{S22}$$

When the separation d is large, one has $S \ll 1$ and obtains two bound states with energies

$$E_\pm = E_s + C \pm D. \tag{S23}$$

Evaluating integrals

To obtain the matrices $\mathbf{S}$, $\mathbf{C}$, and $\mathbf{D}$, we need to evaluate integrals which involve functions centered at two locations with separation d. We first consider the simple case, in which the two impurities are aligned along z instead of the y axis. The result for the latter case can then be obtained via Wigner rotations.

Imagine we have two coordinate systems a and b for which the z-axis coincides with the dimer axis, the x, y axes of the two coordinate systems are parallel to each other, and the origins coincide with the adatom locations. In terms of spherical coordinates, a point in space can be written as (r_a, θ_a, ϕ) and (r_b, θ_b, ϕ). It is convenient to introduce prolate spheroidal coordinates (ξ, η, ϕ), defined by

$$r_a = \frac{\xi + \eta}{2}d, \quad r_b = \frac{\xi - \eta}{2}d, \quad \cos\theta_a = \frac{\xi\eta + 1}{\xi + \eta}, \quad \cos\theta_b = \frac{\xi\eta - 1}{\xi - \eta}, \quad dV = \frac{d^3}{8}(\xi^2 - \eta^2)d\xi d\eta d\phi, \tag{S24}$$

where dV is the volume element.

Denote the Shiba wave function for a single impurity as

$$\phi(\mathbf{r}) = R(r)Y_{lm}(\hat{r}), \tag{S25}$$

where $R(r)$ is a two-component radial wavefunction and the complex spherical harmonics are defined as

$$Y_{lm}(\hat{\mathbf{r}}) = A_{lm} P_{l,m}(cos(\theta)) e^{im\phi}, \quad A_{lm} = \sqrt{\frac{2l+1}{4\pi}\frac{(l-m)!}{(l+m)!}}, \tag{S26}$$

with $P_{l,m}(x)$ the associated Legendre polynomial.

In the following, we first evaluate the integrals with Shiba states as given above. For the case with the two impurities aligned along the z axis, we denote the matrices as $\mathbf{S}'$, $\mathbf{C}'$, and $\mathbf{D}'$.

Overlap integral $\mathbf{S}'$

$$S'_{ab} = \int d\boldsymbol{r}\, \phi_a(\boldsymbol{r})^\dagger \phi_b(\boldsymbol{r} + d\hat{z}) = A_{la,ma} A_{lb,mb} \frac{2\pi d^3}{8} \delta_{ma,mb} I_S(d) \tag{S27}$$

$$I_S(d) = \int_{-1}^{1} d\eta \int_{1}^{\xi^*} d\xi \alpha_S(\eta, \xi; d) \tag{S28}$$

$$\alpha_S(\eta, \xi; d) = R_a(\frac{(\xi+\eta)d}{2})^\dagger R_b(\frac{(\xi-\eta)d}{2}) P_{la,ma}(\frac{1+\xi\eta}{\xi+\eta}) P_{lb,mb}(\frac{\xi\eta-1}{\xi-\eta})(\xi^2-\eta^2) \tag{S29}$$

Coulomb-like integral $\mathbf{C}'$

$$C'_{ab} = \int d\boldsymbol{r}\, \phi_a(\boldsymbol{r})^\dagger \phi_b(\boldsymbol{r}) J(\boldsymbol{r} + d\hat{z}) = A_{la,ma} A_{lbmb} \frac{2\pi d^3}{8} \delta_{ma,mb} I_C(d) \tag{S30}$$

$$I_C(d) = \int_{-1}^{1} d\eta \int_{1}^{\infty} d\xi \alpha_C(\eta, \xi; d) \tag{S31}$$

$$\alpha_C(\eta, \xi; d) = R_a(\frac{(\xi+\eta)d}{2})^\dagger R_b(\frac{(\xi+\eta)d}{2}) P_{la,ma}(\frac{1+\xi\eta}{\xi+\eta}) P_{lb,mb}(\frac{1+\xi\eta}{\xi+\eta}) J(\frac{(\xi-\eta)d}{2})(\xi^2-\eta^2) \tag{S32}$$

Exchange-like integral $\mathbf{D}'$

$$D'_{ab} = \int d\boldsymbol{r}\, \phi_a(\boldsymbol{r})^\dagger \phi_b(\boldsymbol{r} + d\hat{z}) J(\boldsymbol{r}) = A_{la,ma} A_{lbmb} \frac{2\pi d^3}{8} \delta_{ma,mb} I_D(d) \tag{S33}$$

$$I_D(d) = \int_{-1}^{1} d\eta \int_{1}^{\infty} d\xi \alpha_D(\eta, \xi; d) \tag{S34}$$

$$\alpha_D(\eta, \xi; d) = R_a(\frac{(\xi+\eta)d}{2})^\dagger R_b(\frac{(\xi-\eta)d}{2}) P_{la,ma}(\frac{1+\xi\eta}{\xi+\eta}) P_{lb,mb}(\frac{\xi\eta-1}{\xi-\eta}) J(\frac{(\xi+\eta)d}{2})(\xi^2-\eta^2). \tag{S35}$$

We evaluate the two-dimensional integrals I_S, I_C and I_D numerically.

Basis Transformation

So far, we chose the angular-momentum quantization axis for a single-impurity Shiba state parallel to the dimer axis. Let us denote the Cartesian axes of this coordinate system by $x'y'z'$. We now evaluate the integrals in the xyz coordinate system in which the two impurities are aligned along the y-axis as introduced in the Hamiltonian (S14).

The spherical harmonics $|lm\rangle_{x'y'z'}$ in coordinate system $x'y'z'$ are related to the ones $|lm\rangle_{xyz}$ in coordinate system xyz by a rotation $R(\varphi,\theta,\psi)$, where $(\varphi,\theta,\psi)=(0,\pi/2,\pi/2)$ are Euler angles, namely

$$|lm\rangle_{xyz} = R(\varphi,\theta,\psi)\,|lm\rangle_{x'y'z'} = \sum_{m'} D^l_{m'm}(\varphi,\theta,\psi)\,|lm'\rangle_{x'y'z'}\,. \tag{S36}$$

Here, we introduced the Wigner matrix

$$\mathcal{D}^l_{m'm}(\varphi,\theta,\psi) = \langle lm'|\,R(\varphi,\theta,\psi)\,|lm\rangle\,, \tag{S37}$$

which has the property

$$\mathcal{D}^l_{m'm}(\varphi,\theta,\psi) = e^{-i\varphi m'}\mathcal{D}^l_{m'm}(0,\theta,0)e^{-i\psi m}. \tag{S38}$$

In xyz coordinate, the matrices for overlap, Coulomb-like and exchange-like integrals computed above transform into

$$\mathbf{S}^{\text{complex}} = \mathcal{D}^\dagger\mathbf{S}'\mathcal{D} \tag{S39}$$

$$\mathbf{C}^{\text{complex}} = \mathcal{D}^\dagger\mathbf{C}'\mathcal{D} \tag{S40}$$

$$\mathbf{D}^{\text{complex}} = \mathcal{D}^\dagger\mathbf{D}'\mathcal{D}, \tag{S41}$$

where $\mathbf{S}'$, $\mathbf{C}'$, and $\mathbf{D}'$ are the diagonal matrices given in Eqs. (S27, S30, and S33), and the matrix $\mathcal{D}$ has matrix elements

$$(\mathcal{D})_{m'm} = \mathcal{D}^2_{m'm}(\varphi,\theta,\psi), \tag{S42}$$

where α,β,γ are the Euler angles, which rotate $x'\to x$, $y'\to y$ and $z'\to z$.

Furthermore, we are interested in these matrices for the real angular basis as defined in Eq. (S13). In this real basis, we have

$$\mathbf{S} = \mathcal{U}^\dagger\mathbf{S}^{\text{complex}}\mathcal{U} = (\mathcal{D}\mathcal{U})^\dagger\mathbf{S}'\mathcal{D}\mathcal{U} \tag{S43}$$

$$\mathbf{C} = \mathcal{U}^\dagger\mathbf{C}^{\text{complex}}\mathcal{U} = (\mathcal{D}\mathcal{U})^\dagger\mathbf{C}'\mathcal{D}\mathcal{U} \tag{S44}$$

$$\mathbf{D} = \mathcal{U}^\dagger\mathbf{D}^{\text{complex}}\mathcal{U} = (\mathcal{D}\mathcal{U})^\dagger\mathbf{D}'\mathcal{D}\mathcal{U}, \tag{S45}$$

where the matrix $\mathcal{U}$ is given by

$$\mathcal{U} = \begin{pmatrix} \frac{i}{\sqrt{2}} & 0 & 0 & 0 & \frac{1}{\sqrt{2}} \\ 0 & \frac{i}{\sqrt{2}} & 0 & \frac{1}{\sqrt{2}} & 0 \\ 0 & 0 & 1 & 0 & 0 \\ 0 & \frac{i}{\sqrt{2}} & 0 & -\frac{1}{\sqrt{2}} & 0 \\ -\frac{i}{\sqrt{2}} & 0 & 0 & 0 & \frac{1}{\sqrt{2}} \end{pmatrix}, \tag{S46}$$

and the real and complex angular bases are $\{Y_{xy}, Y_{yz}, Y_{z^2}, Y_{xz}, Y_{x^2-y^2}\}$ and $\{Y_{2,-2}, Y_{2,-1}, Y_{2,0}, Y_{2,1}, Y_{2,2}\}$, respectively.

In the following, we use this formalism to discuss the hybridized orbitals, splittings, and shifts for the two possible dimer orientions along the $\langle 110\rangle$ and the $\langle 100\rangle$ directions. The appearance of the hybridized orbitals in STM measurements can also be extracted from the pictorial representation of d orbitals in Figs. S1 and S2.

Dimers aligned along $\langle 110\rangle$ direction

Now we consider the case where the dimers are aligned along the $\langle 110\rangle$ direction, see Fig. S1. We need to take the Euler angles $(\varphi,\theta,\psi)=(0,\pi/2,\pi/4)$, which gives rise to the rotation matrix

$$\mathcal{D} = \begin{pmatrix} \frac{i}{4} & \frac{e^{i\pi/4}}{2} & \frac{\sqrt{6}}{4} & -\frac{e^{i3\pi/4}}{2} & -\frac{i}{4} \\ -\frac{i}{2} & -\frac{e^{i\pi/4}}{2} & 0 & -\frac{e^{i3\pi/4}}{2} & -\frac{i}{2} \\ \frac{\sqrt{6}i}{4} & 0 & -\frac{1}{2} & 0 & -\frac{\sqrt{6}i}{4} \\ -\frac{i}{2} & \frac{e^{i\pi/4}}{2} & 0 & \frac{e^{i3\pi/4}}{2} & -\frac{i}{2} \\ \frac{i}{4} & -\frac{e^{i\pi/4}}{2} & \frac{\sqrt{6}}{4} & \frac{e^{i3\pi/4}}{2} & -\frac{i}{4} \end{pmatrix}. \tag{S47}$$

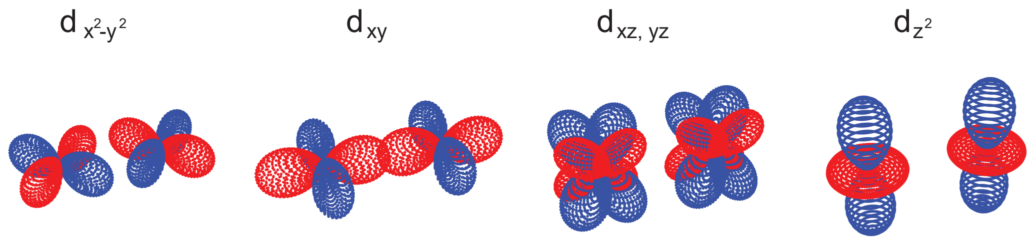

Figure S1. Schematic representation of hybridizing d-orbitals of the two adatoms making up the dimer oriented along the $\langle 110 \rangle$ direction, with blue and red indicating the sign of the wave function. From left to right: $d_{x^2-y^2}$ (α resonance), d_{xy} and $d_{yz,xz}$ (γ resonance), and d_{z^2} (β resonance). For the $\langle 110 \rangle$ dimer, the $d_{yz,xz}$ of the monomers form symmetric and antisymmetric combinations which do not mix under the hybridization between the monomers. Here, we show only one of these linear combinations as their appearance and splittings are essentially the same. Note that the images as observed in STM experiments can be roughly interpreted as a top view onto the resulting hybridized orbitals.

After some algebra, we obtain the overlap matrix

$$\boldsymbol{S} = \begin{pmatrix} \frac{3S_0}{4} + \frac{S_2}{4} & 0 & \frac{\sqrt{3}}{4}\left(S_0 - S_2\right) & 0 & 0 \\ 0 & \frac{S_1}{2} + \frac{S_2}{2} & 0 & -\frac{S_1}{2} + \frac{S_2}{2} & 0 \\ \frac{\sqrt{3}}{4}\left(S_0 - S_2\right) & 0 & \frac{S_0}{4} + \frac{3S_2}{4} & 0 & 0 \\ 0 & -\frac{S_1}{2} + \frac{S_2}{2} & 0 & \frac{S_1}{2} + \frac{S_2}{2} & 0 \\ 0 & 0 & 0 & 0 & S_1 \end{pmatrix}. \tag{S48}$$

Similar expressions for $\mathbf{C}$ and $\mathbf{D}$ also exist and are obtained by simply replacing S by C and D, respectively.

α and β peaks

At large distances, we apply Eq. (S23) and obtain

$$E_{\pm}^{\alpha} = E_s^{x^2-y^2} + C_1^{\alpha} \pm D_1^{\alpha} \tag{S49}$$

$$E_{\pm}^{\beta} = E_s^{z^2} + \frac{(C_0^{\beta} \pm D_0^{\beta}) + 3(C_2^{\beta} - D_2^{\beta})}{4}. \tag{S50}$$

γ peak

Although the γ peak derives from the d_{xy}, d_{yz}, and d_{xz} orbitals, we see from Eq. (S48) that d_{xy} decouples from the others. We consider the large-d case and neglect S. Using Eq. (S23), we obtain

$$E_{xy,\pm}^{\gamma} = E_s^{xy,yz,xz} + \frac{3(C_0^{\gamma} \pm D_0^{\gamma}) + (C_2^{\gamma} \pm D_2^{\gamma})}{4}, \tag{S51}$$

and the eigenstates are symmetric and antisymmetric superposition of the d_{xy} states centered at the two adatoms.

To solve for the remaining eigenstates, one can introduce the new basis $\{|d_+\rangle, |d_-\rangle\}$, with

$$|d_+\rangle = \frac{1}{\sqrt{2}}(|d_{yz}\rangle + |d_{xz}\rangle) \tag{S52}$$

$$|d_-\rangle = \frac{1}{\sqrt{2}}(|d_{yz}\rangle - |d_{xz}\rangle). \tag{S53}$$

In this new basis, $\mathbf{S}$, $\mathbf{C}$ and $\mathbf{D}$ become diagonal when restricted to the subspace spanned by $|d_{yz}\rangle$ and $|d_{xz}\rangle$. Thus, the $|d_+\rangle$ and $|d_-\rangle$ states in one adatom couple independently to the same states in the other adatom. We then obtain the energies

$$E_{+,\pm}^{\gamma} = E_s^{xy,yz,xz} + C_2^{\gamma} \pm D_2^{\gamma} \tag{S54}$$

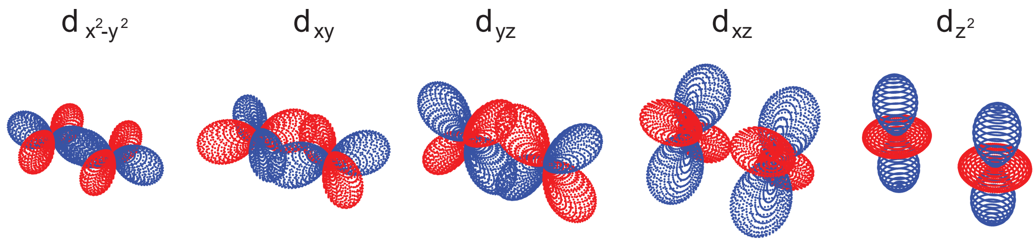

Figure S2. Schematic representation of hybridizing d-orbitals of the two adatoms making up the dimer oriented along the $\langle 100\rangle$ direction, with blue and red indicating the sign of the wave function. From left to right: $d_{x^2-y^2}$ (α resonance), d_{xy}, d_{yz}, d_{xz} (γ resonance), and d_{z^2} (β resonance). For the $\langle 100\rangle$ dimer, the d_{xy}, d_{yz}, and d_{xz} orbitals of the monomers do not mix under the hybridization between the monomers. Moreover, the dimer-induced splitting of the d_{xy} and the d_{yz} orbitals are (approximately) equal, while the hybridization of the d_{xz} orbitals is small, leaving it unshifted and unsplit within our experimental resolution. Note that the images as observed in STM experiments can be roughly interpreted as a top view onto the resulting hybridized orbitals.

of the bound states, which correspond to symmetric and antisymmetric superpositions of d_+ states centered at the two adatoms, and the energies

$$E^{\gamma}_{-,\pm} = E_s^{xy,yz,xz} + C_1^{\gamma} \pm D_1^{\gamma}, \tag{S55}$$

for the eigenstates which are symmetric and antisymmetric superposition of d_- states centered at the two adatoms.

Dimers aligned along y-axis ($\langle 100\rangle$)

Now we consider the case where the dimers are aligned along the $\langle 100\rangle$ direction, see Fig. S2. In this case, we have $(\varphi, \theta, \psi) = (0, \pi/2, \pi/2)$. Thus,

$$\mathcal{D} = \begin{pmatrix} 1/4 & 1/2 & \sqrt{6}/4 & 1/2 & 1/4 \\ -1/2 & -1/2 & 0 & 1/2 & 1/2 \\ \sqrt{6}/4 & 0 & -1/2 & 0 & \sqrt{6}/4 \\ -1/2 & 1/2 & 0 & -1/2 & 1/2 \\ 1/4 & -1/2 & \sqrt{6}/4 & -1/2 & 1/4 \end{pmatrix}, \tag{S56}$$

which gives rise to

$$\boldsymbol{S} = \begin{pmatrix} S_1 & 0 & 0 & 0 & 0 \\ 0 & S_1 & 0 & 0 & 0 \\ 0 & 0 & \frac{S_0+3S_2}{4} & 0 & \frac{\sqrt{3}(S_0-S_2)}{4} \\ 0 & 0 & 0 & S_2 & 0 \\ 0 & 0 & \frac{\sqrt{3}(S_0-S_2)}{4} & 0 & \frac{3S_0+S_2}{4} \end{pmatrix} \tag{S57}$$

Here $S_i = S'_{ii}$ are integrals defined in Eq. (S27) using complex spherical harmonics in the $x'y'z'$ coordinate system. Similar expressions for $\mathbf{C}$ and $\mathbf{D}$ also exist, by replacing S_i by $C_i = C'_{ii}$ and $D_i = D'_{ii}$, which are given in Eqs. (S30,S33). We also used the relations $S_i = S_{-i}$, $C_i = C_{-i}$ and $D_i = D_{-i}$. Now, we are in a position to analyze the α, β, and γ peaks separately.

α and β peaks

Since the α and β peaks derive from $d_{x^2-y^2}$ and d_{z^2}, respectively, we use Eq. (S21) to compute the bound-state energy of the dimer. The corresponding matrix elements are

$$S_{x^2-y^2,x^2-y^2} = \frac{3S_0+S_2}{4} \tag{S58}$$

$$S_{z^2,z^2} = \frac{S_0+3S_2}{4}. \tag{S59}$$

Similar expressions also exist for C and D. Note that the integrals S_i, C_i and D_i depend on the radial wave functions, which are different for the different states.

At large distance, i.e., when the overlap integrals can be neglected, one can apply Eq. (S23). We have

$$E_{\pm}^{\alpha} = E_s^{x^2-y^2} + \frac{3(C_0^{\alpha} \pm D_0^{\alpha}) + (C_2^{\alpha} \pm D_2^{\alpha})}{4}, \tag{S60}$$

$$E_{\pm}^{\beta} = E_s^{z^2} + \frac{(C_0^{\beta} \pm D_0^{\beta}) + 3(C_2^{\beta} \pm D_2^{\beta})}{4}, \tag{S61}$$

where the subscripts α, β were added to distinguish the integrals computed for the two situations.

γ peak

Since the γ peak derives from the d_{xy}, d_{yz}. and d_{xz} orbitals, we need to solve the generalized eigenvalue equation given in Eq. (S17), taking into account all three states on each adatom. However, from Eq. (S57), we see that the d_{xy}, d_{yz}, and d_{xz} states decouple from each other, with

$$S_{xz,xz}, C_{xz,xz}, D_{xz,xz} = S_2, C_2, D_2, \tag{S62}$$

and

$$S_{xy,xy}, C_{xy,xy}, D_{xy,xy} = S_{yz,yz}, C_{yz,yz}, D_{yz,yz} = S_1, C_1, D_1. \tag{S63}$$

Hence, we can directly apply Eqs. (S21) and (S23) to compute the bound-state energy of the dimer. At large distance, we have

$$E_{xz,\pm}^{\gamma} = E_s^{xy,yz,xz} + C_2^{\gamma} \pm D_2^{\gamma}, \tag{S64}$$

$$E_{xy,\pm}^{\gamma} = E_{yz,\pm}^{\gamma} = E_s^{xy,yz,xz} + C_1^{\gamma} \pm D_1^{\gamma}. \tag{S65}$$

NUMERICAL RESULTS

For illustration, we present some numerical result. A full numerical implementation for realistic parameters is too demanding in view of the large ratio between coherence length and Fermi wavelength. Since the dimer dimension is very small compared to the coherence length, we keep realistic values for the Fermi wavelength, but reduce the coherence length significantly (while leaving it larger than the Fermi wavelength) by choosing an unrealistically large gap Δ. Moreover, we also truncate k such that

$$\frac{\alpha_{k,l}^2}{2R^2} \leq E_F + \epsilon. \tag{S66}$$

The cutoff ϵ should be chosen large compared to Δ, but in practice, we choose it of order Δ, so that the necessary basis set does not become too large. As a result, our numerical calculations generate reasonable d-orbital-like Shiba wave functions within the superconducting gap whose hybridization can then be studied within the variational approximation discussed above. The calculations provide qualitative insights into the hybridization but do not suffice for quantitative predictions.

Specifically, we take an unrealistically large superconducting gap of $\Delta = 500$ meV, but the Fermi energy $E_F = 9470$ meV for Pb, corresponding to a Fermi wavelength of $\lambda_F = 3.99$ Å. We require the radius R of the finite simulation space defined in Eq. (S5) large enough, such that the level spacing (at fixed angular momentum) due to the finite size quantization is much smaller than the superconducting gap, namely $R \gg \sqrt{\mu}/\Delta$. We choose $R = 761$ Å in order to fulfill this requirement. Furthermore, we choose the cutoff ϵ in Eq. (S66) to be 250 meV, and an exchange potential

$$J(r) = \frac{V}{\sqrt{\pi} a} \exp\left(-\frac{r^2}{a^2}\right), \tag{S67}$$

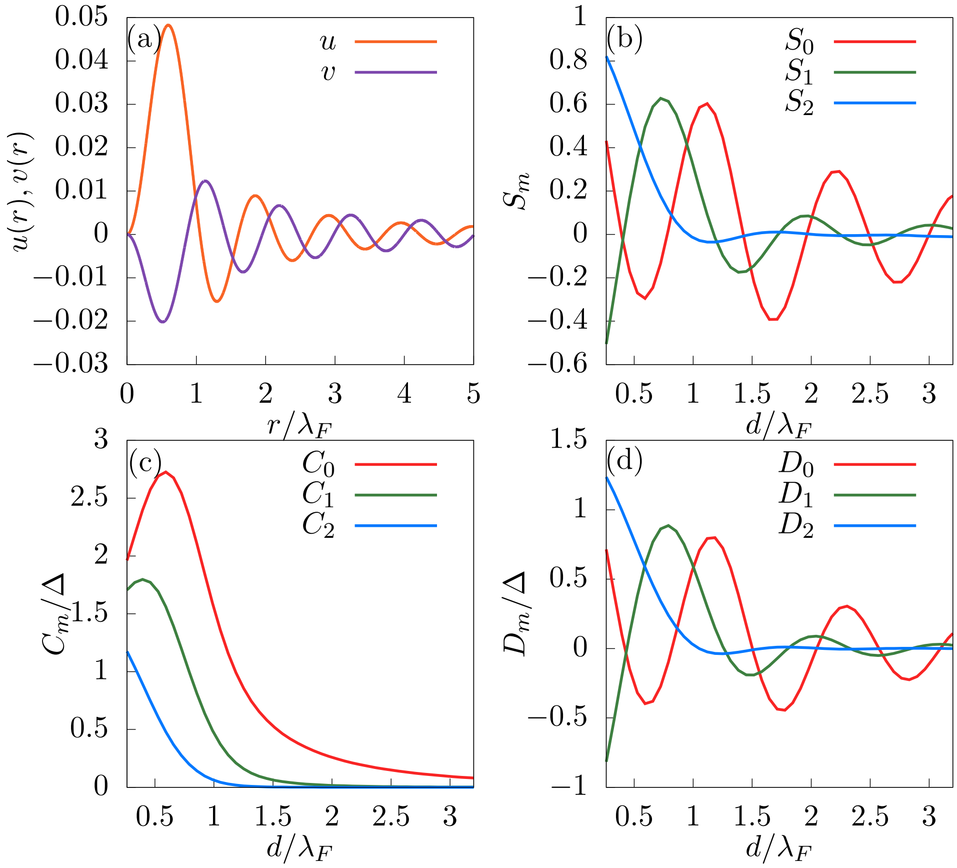

Figure S3. (a) The radial part of the Shiba state wave function. The electron and hole components are denoted as $u(r)$ and $v(r)$ respectively. (b–d) Overlap, Coulomb-like, and exchange-like integrals in terms of complex spherical harmonics with magnetic quantum number m.

where a and V characterize the range and the strength of the potential. Note that in the limit $a \to 0$, $J(r) \to V\delta(r)$. We choose $a = 1.59$ Å and $V = 122000$ meV in order to produce Shiba states in the $l = 2$ sector with energy $E_s = 0.4274\Delta$.

In Fig. S3(a), we show electron and hole components of the radial Shiba state wave function, denoted as $u(r)$ and $v(r)$. In Figs. S3(b–d), we show S_m, C_m and D_m for $m = 0, 1, 2$, which are used in computing the Shiba states energies for two impurities. The energies of Shiba states with two magnetic impurities oriented along $\langle 110 \rangle$ and $\langle 100 \rangle$ directions are shown in Figs. S4 and S5, respectively.

[1] M. Ruby, Y. Peng, F. von Oppen, B.W. Heinrich, and K.J. Franke, Phys. Rev. Lett. **117**, 186801 (2016).

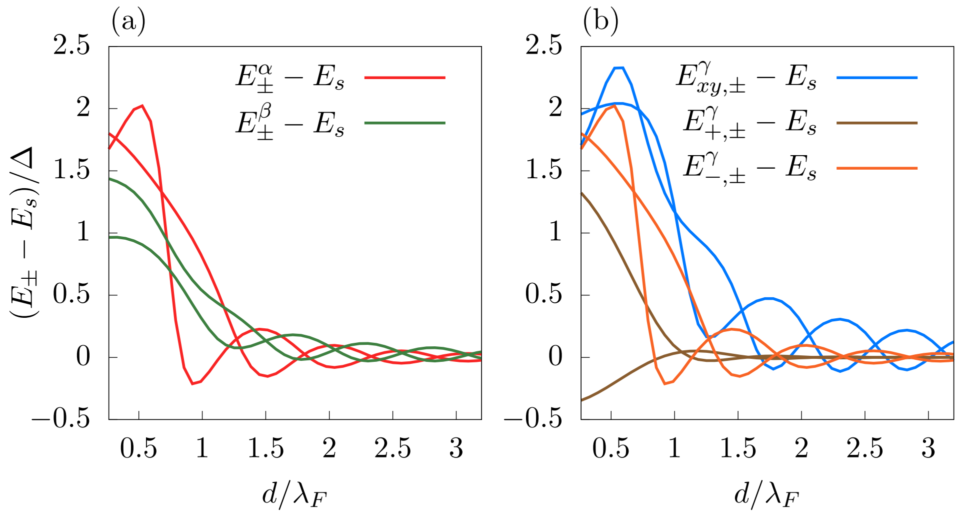

Figure S4. The energy of Shiba states with two magnetic impurities oriented along $\langle 110 \rangle$ direction, measured from the Shiba state energy of an isolated impurity, originated from different d orbitals. These states can be identified as α, β and γ peaks according to the STM measurement. (a) α, β peaks. (b) γ peak.

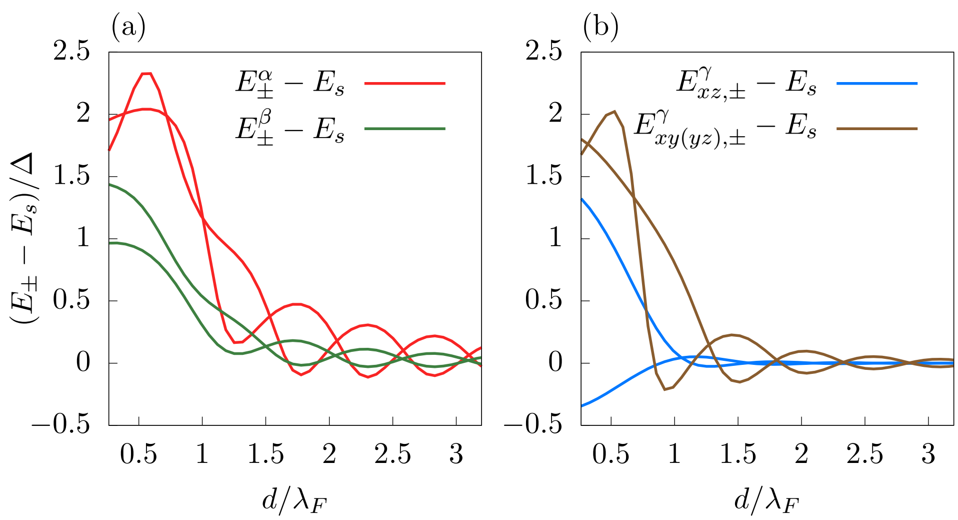

Figure S5. The energy of Shiba states with two magnetic impurities oriented along $\langle 100 \rangle$ direction, measured from the Shiba state energy of an isolated impurity, originated from different d orbitals. These states can be identified as α, β and γ peaks according to the STM measurement. (a) α, β peaks. (b) γ peak.